



SEASONAL AMBIENT NOISE LEVELS IN ICE-COVERED WATERS OF THE NANSEN BASIN

Dag Tollefsen* Lars Ødegaard Vidar Forsmo
Norwegian Defence Research Establishment (FFI), Horten, Norway

ABSTRACT

This paper presents analysis of 1-year (2019–2020) passive acoustic recordings of underwater ambient noise (40 Hz–2 kHz) at an ice-covered location in the Nansen Basin of the Arctic Ocean. A deep-water multi-institution rig (maintained by the EU-INTAROS project) was deployed and retrieved by the icebreaker KV SVALBARD. The rig included an acoustic recorder fitted with a single hydrophone at 1000 m depth. Time series of ambient noise show highest correlations with wind speed, air temperature, and ice concentration. Multivariate regression models are fitted to data to quantify the environment parameter dependence of ambient noise in under-ice conditions.

Keywords: *ambient noise, Arctic, soundscape.*

1. INTRODUCTION

Historic low-frequency acoustic measurements in the Arctic (see [1] for an overview) illuminated the specifics Ambient Noise (AN) due to ice conditions. The sea ice extent has reduced over the past decades and now comprises younger and thinner ice, which in turn affects noise-generating processes. In addition, changes in oceanographic structure, e.g., seasonal occurrence of a subsurface sound speed duct, can allow distant-generated noise to impact AN. The number of reported recent data sets from the Arctic is increasing with efforts to model the environment factor influence on AN ongoing [2-5]. Regression equations that relate AN to wind speed are well-established for open water [6] but has to date been less explored for ice-covered

*Corresponding author: dag.tollefsen@ffi.no.

Copyright: ©2023 This is an open-access article distributed under the terms of the Creative Commons Attribution 3.0 Unported License, which permits unrestricted use, distribution, and reproduction in any medium, provided the original author and source are credited.

waters. We present a one-year data set from the Nansen Basin of the Arctic Ocean (section 2). We explore environmental parameter dependence via linear regression analysis (section 3). Section 4 contains a summary.

2. DATA AND PROCESSING

Acoustic data were collected by FFI using an AMAR instrument (Jasco Applied Sciences, Canada) fitted in-line to a multi-institution rig maintained under the INTAROS project.¹ The rig was bottom-moored at 3850 m water depth at position 81° 47' N 022° E, 60 nmi north of the Svalbard archipelago. The site is within the Nansen Basin

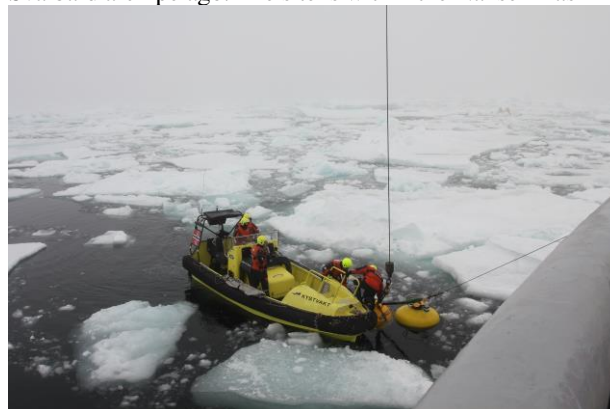


Figure 1. Recovery of deep-water mooring in the ice-covered Nansen Basin on July 24, 2020.

of the Arctic Ocean (Eurasian Basin). The rig was deployed and recovered in ice-covered waters on Sep. 3, 2019 and July 24, 2020 (Fig. 1), respectively, by the Norwegian Coast Guard icebreaker KV SVALBARD. A seasonal cover of predominantly first-year ice characterizes ice conditions in the area. Observations of

¹ <https://cordis.europa.eu/project/id/727890>

marine mammals north of Svalbard include bowhead whale, ringed seal, bearded seal and walrus; seasonal presence of larger cetaceans include fin and blue whale [7], while signals due to sperm and bowhead whale have been observed in the Fram Strait. Shipping activity due to fishing and tourism is sporadic in periods of ice-free waters [8].

included OSI-SAF Global Sea Ice data (12.5 km grid) for daily mean sea ice concentration, and the AROME Arctic weather model (2.5 km/3 hr resolution) for air pressure and temperature, wind speed, and ocean current profiles.

3. RESULTS

3.1 LTS and ice conditions

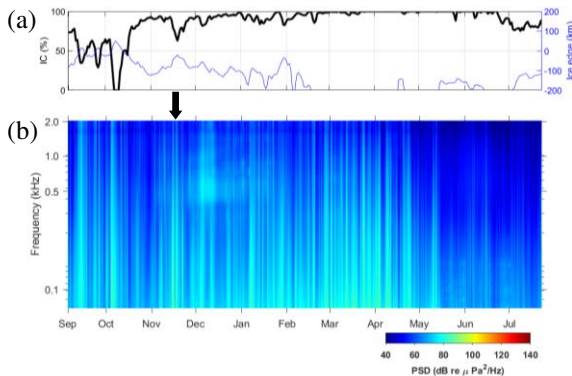


Figure 2. (a) Daily ice concentration at sensor (in %, black line) and range to the ice edge (in km, blue line); (b) Long-term spectrogram 40 Hz–2 kHz (dB re $\mu\text{Pa}^2/\text{Hz}$). Nansen Basin 2019–2020 dataset.

We collected acoustic data with a M5-V30-100 hydrophone (GeoSpectrum Inc., Canada) attached to an AMAR-G4-UD recording instrument. The hydrophone sensitivity was -164.3 dB re 1 V/ μPa with a high-pass filter at 10 Hz before 24-bit digitization. To limit power consumption, the instrument (D-cell battery powered) was set to record at 33% duty cycle: 16 kHz sampling for 20 min. each 2 of 3 hours, and 64 kHz for 20 min. each 3rd hour during 1 yr. Time scheduling was implemented so that recording did not overlap with active acoustic instruments (up- and downward looking ADCPs) mounted on the same rig. For noise power spectral density (PSD) estimation, we used the Welch method with 1-min averages over 1 s FFT samples (Hamming windowed with 50% overlap). This resulted in 480 one-minute noise spectra per day. Resulting PSD noise levels (NL) are in units of dB re 1 $\mu\text{Pa}^2/\text{Hz}$. To estimate a persistent background noise level, we processed data by a procedure adopted from Kinda [3]. We then used short-term FFTs (sliding time window length 64 ms and 50% overlap) over the first 7 min of data from each hour. The resulting Ambient Noise Levels (ANL) in dB re 1 $\mu\text{Pa}^2/\text{Hz}$ were estimated from the lowest 15th percentile of each frequency bin. We accessed environmental data from the Norwegian Meteorological Institute (met.no) [9]. This

Fig. 2(a) shows daily ice concentration (IC) at the sensor location (in %) and range to the ice edge (in km, defined by 15% IC). There is *nearly full ice cover* (IC >95%) from mid-December to mid-June. Fig. 2(b) shows the long-term spectrogram (LTS) (NL in the frequency band 40 Hz–2 kHz). The LTS displays seasonality observed in ice-covered waters: high NL during periods of open water and partial ice cover, and lower NL (by 15–20 dB) in periods of high IC. Note also intermittent shorter-term periods of elevated NL (by 6–12 dB), e.g., in mid-November and in March. For example, the event on Nov 15–17 (black arrow) coincides with the icebreaker R/V Kronprins Haakon operating in the area; data from this period were excluded from further analysis. Note also a band (0.4–1 kHz) of elevated NL from November through February, attributed to presence of marine mammals (bearded seal). These signals are of intermittent occurrence hence effectively suppressed when using ANL processing.

3.2 Correlation analysis

We applied correlation analysis to hourly time series of broadband ANL (power-sum over the decadal frequency band 0.1–1 kHz) and environmental factors (data taken from met.no models at the nearest grid position and up-sampled to 1-hr resolution). For the 275-day data set, the highest correlations were with wind speed, v , in m/s, at 10 m height (Pearson's correlation coefficient $r = 0.39$) and air temperature, T , ($r = -0.30$), followed by IC ($r = -0.16$), air pressure, p_{air} , ($r = -0.16$) and ocean surface current ($r = 0.12$) [all p-values < 0.01]. Alternative parameterizations for ice conditions, including IC within a 100-km radius, as well as time lags (up to ± 1 day) between ANL and environmental factors did not significantly alter the correlations over those reported here.

3.3 Regression model

Expanding on noise models for open water, we propose a log-wind speed dependent model:

$$ANL = O + 20 \cdot n \log_{10} v + \sum_k \alpha_k \theta_k \quad (1)$$

with ANL the broadband ambient noise level (in dB re μPa^2), O an offset parameter, n the slope of the log-dependence on wind speed v . Further terms are coefficients α_k of additional environment parameters θ_k of a linear model. The model is fitted using least-squares multivariate linear regression implemented in MATLAB. To distinguish data between differing ice conditions, we subdivided data into: (a) IC 5–95%, and (b) IC>95%; the 2nd category taken to represent *nearly full ice cover*. This differs slightly from categorizations used in previous work [2,5] but was found convenient for the present data set. The multivariate linear regression model for IC 5–95% data is estimated as

$$ANL = 80.5 + 0.700 \cdot 20 \log_{10} v - 0.165 \cdot IC - 0.265 \cdot T \quad (2)$$

while the model for IC>95% data is estimated as

$$ANL = 71.7 + 0.444 \cdot 20 \log_{10} v - 0.242 \cdot T. \quad (3)$$

The number of model parameters (the model order, k) is here determined using the Bayes Information Criterion (BIC) [10]. Assuming Gaussian errors and using the maximum likelihood estimate for data error variances, the BIC is

$$BIC = M \log N + N \log(RSS / N) \quad (4)$$

where $M=k+2$ is the number of model parameters (model order k), N is the number of data, and RSS the residual sum of squares. For the IC 5–95% data, $k=3$ yielded a minimum for the BIC [the Eqn. (2) model]. For the IC>95% data, $k=2$ yielded a minimum for the BIC [the Eqn. (3) model]. Note that the wind speed dependence is significantly reduced (by ~40%) from intermediate (IC 5–95%) to high IC (IC>95%). This fits with earlier results on wind-driven noise in ice-covered waters [2–5]. Table 1 shows test statistics for the $k=1-5$ models for IC 5–95% data. The table shows that using the p-value as criteria for model selection suggests including all five parameters in the model. However, the r and the std criteria shows that the 4th and 5th parameters do not give any improvement of the model performance. Fig. 3 shows the model performance in terms of estimated vs. measured ANL for all data samples.

Table 1. Model coefficients, in order of significance, for regression model fits to ANL

(0.1–1 kHz) data for IC 5–95%. The columns are model order k , parameter, p-value test results on parameter significance, the BIC, correlation r between measured and estimated ANL and standard deviation std [dB] of model error.

k	Parameter	p	BIC	r	std
	O	<0.01	10.9e3	0.00	5.68
1	n	<0.01	10.1e3	0.47	5.00
2	IC	<0.01	9.84e3	0.53	4.81
3	T	<0.01	9.22e3	0.63	4.34
4	current	<0.01	9.22e3	0.65	4.34
5	p_{air}	<0.01	9.22e3	0.65	4.34

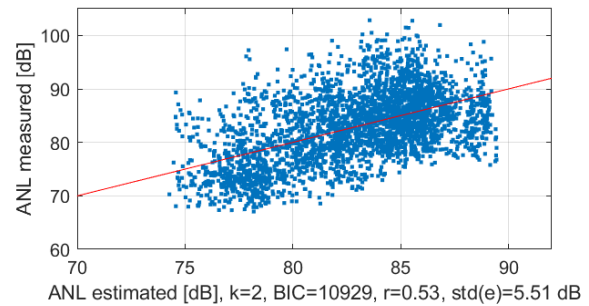
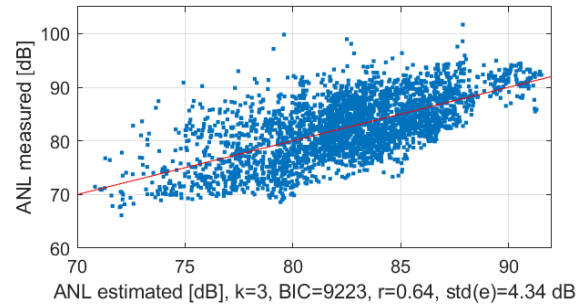


Figure 3. Estimated vs. measured ANL (0.1–1 kHz) for IC 5–95% data (upper panel) and IC>95% data (lower panel) for the BIC selected model. The parameters are $\{v, IC, T_{\text{air}}\}$ for the IC 5–95% model, and $\{v, T_{\text{air}}\}$ for the IC>95% model.

Fig. 4 shows histograms of the residuals. The models assume Gaussian errors, and the figure shows that this is a reasonable assumption. Although we removed data samples where a noisy icebreaker operated in the area and

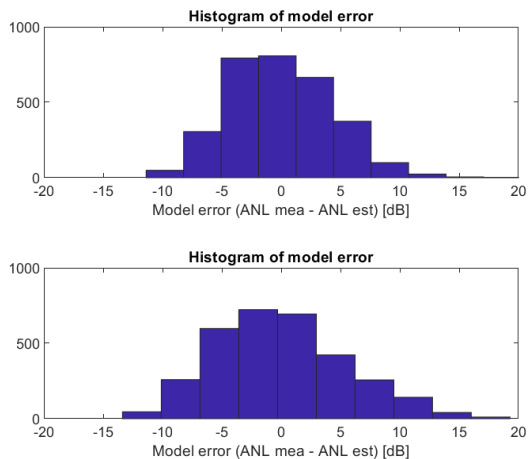


Figure 4. Histogram of ANL model errors for the 5–95% IC (upper) and IC > 95% model (lower).

used the lowest 15th percentile ANL data to suppress biological sounds, it is still a few more positive than negative errors.

4. SUMMARY

This paper examined ambient noise data collected under seasonal ice cover at a deep-water site in the Nansen Basin of the Arctic Ocean. The long-term spectrogram showed typical seasonal dependence with ice concentration: high NL during periods of low IC and lower NL (by 15–20 dB) in periods of high IC. Regression models with log-wind speed dependence and additional environment parameters were used to model data, with the BIC used for model selection. For intermediate ice concentration (IC 5–95%) ANL (0.1–1 kHz) data, a three-parameter model (wind speed, IC, and air temperature) was selected and yielded reasonably good model-data correlation. For high ice concentration (IC > 95%) ANL data, a two-parameter model (wind speed and air temperature) was selected. The wind-speed dependence reduced by ~40% for high IC, consistent with a shielding effect of the ice cover on surface-generated noise. Further work will augment the model with additional parameters observed to affect NL in the marginal ice zone, e.g., wind direction and range to the ice edge. The data set may provide a reference for underwater noise levels in this part of the Arctic Ocean.

ACKNOWLEDGMENTS

The Norwegian Coast Guard icebreaker KV SVALBARD for assistance in rig deployment and recovery. The deep-water rig was maintained by NERSC and IOPAN under the INTAROS project funded by the EU.

REFERENCES

- [1] P. F. Worcester, M. A. Dzieciuch, and H. Sagen, “Ocean acoustics in the rapidly changing Arctic,” *Acoustics Today*, 16, 55–64, 2020.
- [2] E. Roth, J. A. Hildebrand, and S. M. Wiggins, “Underwater ambient noise on the Chukchi Sea continental slope from 2006–2009,” *J. Acoust. Soc. Am.*, 131, 104–110, 2012.
- [3] G. B. Kinda, Y. Simard, C. Gervaise, J. I. Mars, and L. Fortier, “Under-ice ambient noise in Eastern Beaufort Sea, Canadian Arctic, and its relation to environmental forcing,” *J. Acoust. Soc. Am.*, 134, 77–87, 2013.
- [4] J. Bonnel, G. B. Kinda, and D. P. Zitterbart, “Low-frequency ocean ambient noise on the Chukchi Shelf in the changing Arctic,” *J. Acoust. Soc. Am.*, 149, 4061–4072, 2021.
- [5] D. Tollefsen and H. Buen, “Wind- and tidal driven ambient noise in seasonally ice-covered waters north of the Svalbard archipelago,” *JASA Express Lett.*, 2, 086001, 2022.
- [6] W. M. Carey and R. B. Evans, *Ocean Ambient Noise*, Springer, 2011.
- [7] H. Ahonen, K. M. Stafford, C. Lydersen, C. L. Berchok, S. E. Moore, and K. M. Kovacs, “Interannual variability in acoustic detection of blue and fin whale calls in the Northeast Atlantic High Arctic between 2008 and 2018,” *Endang. Species Res.*, 45, 209–224, 2021.
- [8] A. N. Stocker, A. H. H. Renner, and M. Knol-Kauffman, “Sea ice variability and maritime activity around Svalbard in the period 2012–2019,” *Nature: Scientific Reports*, 10, 17043, 2020.
- [9] <https://docs.api.met.no/doc/thredds.html> [Last viewed: April 22, 2023].
- [10] J. K. Ó Ruanaidh and W. J. Fitzgerald, *Numerical Bayesian Methods Applied to Signal Processing*, Berlin: Springer, 1996.